Macromolecular Rapid Communications
www.mrc-journal.de

P-Type Low-Molecular-Weight Hydrogelators

Emily R. Draper, Bart Dietrich, Christopher Brasnett, Stephen Sproules, Tom O. McDonald, Annela M. Seddon, and Dave J. Adams**

As the use of low-molecular-weight gelators (LMWGs) as components in single and multicomponent systems for optoelectronic and solar cell applications increases, so does the need for more functional gelators. There are relatively few examples of p-type gelators that can be used in such systems. Here, the synthesis and characterization of three amino-acid-functionalized p-type gelators based on terthiophene, tetrathiafulvalene, and oligo(phenylenevinylene) are described. The cores of these molecules are already used as electron donors in optoelectronic applications. These newly designed molecules can gel water to form highly organized structures, which can be dried into thin films that show p-type behavior.

1. Introduction

P-type materials have the ability to donate an electron, making them very useful for electronic applications, sensors, p–n heterojunctions and other such devices.[1] Gelation using small molecules has been shown to be an effective way of self-assembling these electronically active materials into highly ordered long-range assemblies.[2] This is advantageous as the self-assembled structures can act like molecular wires, often called nanowires, with charges traveling in one direction.[3] This can even be enhanced further by aligning the gel fibers by shear giving directionally dependent activity.[4] Gelation also offers the possibility of covering large areas, 3D-printing and, spatially resolved patterned surfaces.[5] Depending on the method, gelation can allow access to various different stacking types, aggregation, morphologies, and so different behaviors and activities can be achieved from the same material.[6] Gelation in water in particular opens up different methods in which gelation can be carried out, for example heating and cooling, addition of a salt, changing the pH, and adjusting the solvent environment.[7]

We have shown that a slow change in pH using the hydrolysis of glucono-∂-lactone (GdL) has been shown to give highly reproducible gelation for a range of gelators;[8] reproducibility is key if gelation is to be used to prepare devices. Another advantage of this slow hydrolysis is the possibility of introducing another component that also gels into the system and being able to co-assemble or self-sort the molecules.[9] Not only is this controlled by the pK_a of the molecules and the similarity of the structures,[5a,10] but also by the speed at which gelation is carried out.[10b] Self-sorting leads to the two molecules assembling into two different types of functional fiber that can interact in the gel network. This would be ideal for p–n heterojunctions.[11] Co-assembled fibers, where the different molecules mix in the same fibers, can lead to the sample having completely different properties than either of the individual components.[12] This level of control is very difficult to achieve using other methods of gelation such as heating and cooling, although there are examples where this is possible.[13]

A number of p-type organogelators have been prepared.[3b,14] However, there are currently relatively few examples of p-type hydrogelators in the literature.[15] Here we show the synthesis of three p-type gelators, functionalized with amino acids, or dipeptides. They are based on terthiophene (**1**), tetrathiafulvalene (**2**) and oligo(phenylenevinylene) (**3**) and shown in **Figure 1**a. These gelators can be dissolved in water at high pH, due to the deprotonation of the terminal carboxylic acid of the amino acids. The p-type gels are then formed by lowering the pH of the solutions using GdL. The structures formed at high pH and low pH are analyzed by UV–vis absorption spectroscopy, rheology, X-ray scattering, and SEM. We then describe their ability to act as p-type materials by analyzing their conductivity under iodine vapor.

2. Experimental Section

Full characterization and synthetic procedures are provided in the Supporting Information, along with the other experimental protocols.

Dr. E. R. Draper, Dr. B. Dietrich, Dr. S. Sproules, Prof. D. J. Adams
School of Chemistry
University of Glasgow
Glasgow G12 8QQ, UK
E-mail: Emily.Draper@glasgow.ac.uk; Dave.Adams@glasgow.ac.uk
C. Brasnett, Dr. A. M. Seddon
School of Physics
HH Wills Physics Laboratory
University of Bristol
Bristol BS8 1FD, UK
Dr. T. O. McDonald
Department of Chemistry
University of Liverpool
Liverpool L69 7ZD, UK
Dr. A. M. Seddon
Bristol Centre for Functional Nanomaterials
School of Physics
HH Wills Physics Laboratory
University of Bristol
Bristol BS8 1FD, UK
The ORCID identification number(s) for the author(s) of this article can be found under https://doi.org/10.1002/marc.201700746.

DOI: 10.1002/marc.201700746

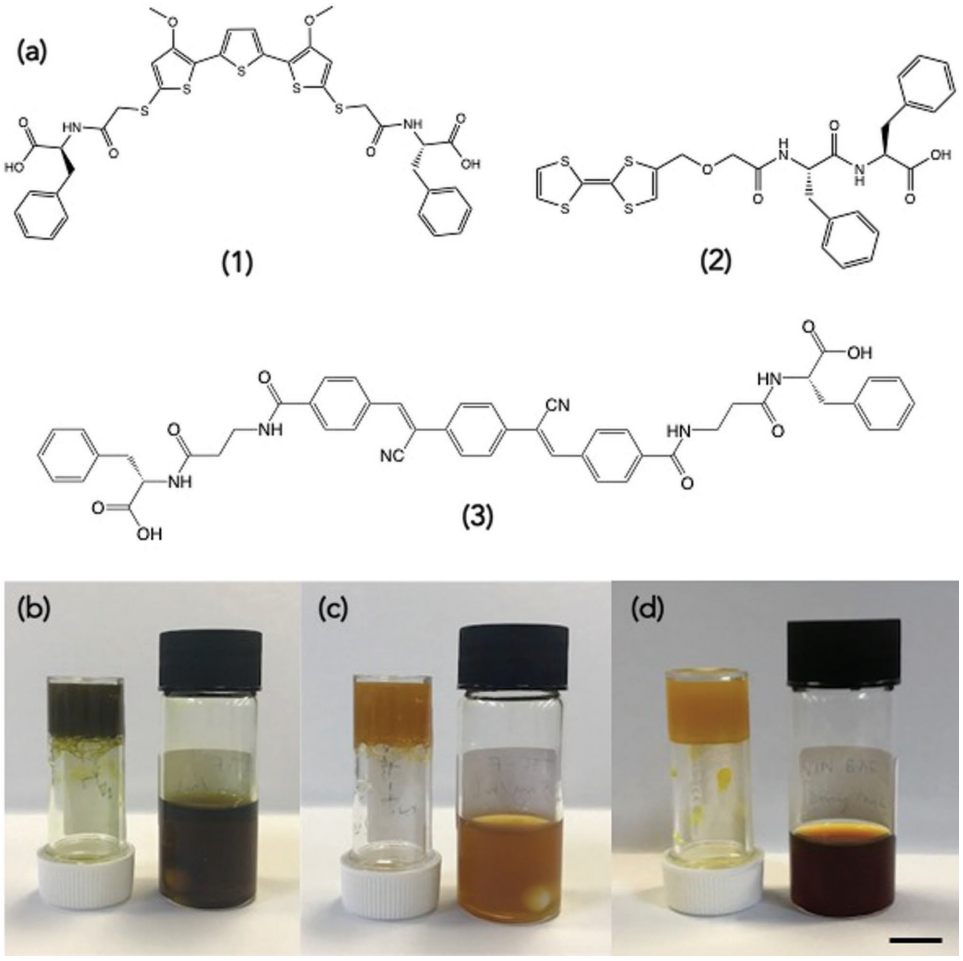

Figure 1. a) Chemical structure of gelators 1, 2, and 3. Photographs of the solutions at pH 8 (1 and 2) and pH 10 (3) (left) and the resulting gel at low pH of b) 1, c) 2, and d) 3. Scale bar represents 1 cm.

3. Results and Discussion

Solutions of **1** and **2** were prepared at a concentration of 5 mg mL^{-1} and **3** at a concentration of 10 mg mL^{-1} (**3** had a higher minimum gelation concentration than **1** and **2** and so did not form a gel at 5 mg mL^{-1}) in water. **2** needed 1 equivalent of 0.1 M NaOH and **1** and **3** required 2 equivalents of 0.1 M NaOH in order to deprotonate the carboxylic groups and become soluble in water. This results in solutions with a pH of 8 (solutions **1** and **2**) or 10 (solution **3**). All solutions were free-flowing with a yellow/brown color. Viscosity measurements of solutions of **1** and **3** showed that these were not viscous and showed little or no shear thinning behavior suggesting there is little structure in the solutions. As the viscosity of the samples is so low, this leads to noisy data at low shear rates as seen for solution **3**. (Figure S1a–c Supporting Information). The solution of **2** was found to be much more viscous than the other two samples and showed shear thinning behavior indicating the presence of worm-like micelles in solution (Figure S1b, Supporting Information).[12]

The solutions at high pH were characterized by small angle X-ray scattering (SAXS). The solution of **1** at high pH scatters weakly (Figure S2a, Supporting Information). The data at high Q can fit to a sphere model, with the fit suggesting a radius of 1.52 ± 0.04 nm. These data suggest that **1** exists primarily as free molecules at high pH, which is consistent with the viscosity data (above). At high pH, the solution of **2** scatters much more strongly than the solutions of either **1** or **3**. The scattering data for the solution of **2** (Figure S2a, Supporting Information) are best fitted to an elliptical cylinder with a radius of 3.24 ± 0.03 nm, a radius ratio of 4.07 ± 0.01, and a length of 418.4 ± 30.2 nm. Again, this agrees with the high viscosity of the solution of **2** as compared to that of **1** or **3**. The solution of **3** at high pH scatters weakly (Figure S2c, Supporting Information). As for **1**, the data at high Q can be fitted to a sphere model, with a radius of 1.82 ± 0.03 nm. The scattering at low Q is effectively a power law. We have observed similar data previously for an oligo(phenylvinylene)-based gelator at high pH,[15d] and we assigned the data to the coexistence of free molecules (which scatter like spheres) and a small fraction of weakly scattering worm-like micelles. This too would be consistent with the viscosity data (see above). Scanning electron microscopy (SEM) was used to image dried solutions of **1**–**3**. No defined structures could be imaged for solutions **1** or **3** which agree with the scattering and viscosity data that also suggest the lack of persistent self-assembled

species at this pH. The solution of **2** showed the presence of fibrous like structures, but due to the size of the structures and drying effects they were not very clear (Figure S3, Supporting Information).[16]

To form gels, 2 mL of each solution was added to a vial containing 10 mg of GdL. The solution and GdL were shaken gently to ensure the GdL had dissolved. The samples were then left overnight to gel. This resulted in samples that were stable to inversion with a pH of around 3.3. Strain and frequency sweeps were then performed on the gels. **1**, **2**, and **3** were found to form gels with very reproducible rheological properties (Figures S4–S6, Supporting Information). All gels broke with strain and showed little dependence on frequency which is typical for low molecular weight gels.[17] Gel **1** was found to have the highest storage modulus (*G′*) and loss modulus (G″) of 8000 and 1000 Pa, respectively. The gel began to yield at 3% strain and flowed at 30% strain (Figure S4 and Table S1, Supporting Information). Gel **3** was the weakest, with a *G′* and *G″* of 300 and 30 Pa, respectively and yielded at 10% strain (Figure S6 and Table S1, Supporting Information).

The gelation kinetics were measured along with the change in pH (Figures S7–S9, Supporting Information). All three gels showed different gelation kinetics; typically these are dependent on the pK_a of the assembled gelators as we have shown before for related gels.[10b,17a] An increase in both *G′* and G″ starts when the pH reaches that of the apparent pK_a of the self-assembled structure.[8a,17a] *G′* and *G″* evolve in different stages, driven by the changes in pH, before reaching a plateau. For example, **1** started to gel after 20 min (as shown by *G′* and *G″* starting to increase) when the pH of the system was at 6.2, which is consistent with the measured pK_a of the system. There is a second increase of *G′* and *G″* at 100 min, indicating another stage of assembly has started to occur as we have seen in other LMWGs (**Figure 2**a; Figure S7, Supporting information).[5a] The sample was completely gelled after 17 h when the system was at pH 3.1. **2** started to assemble at pH 7.2 (around the pK_a) and had more steps in the assembly after 70 min and 100 mins where *G′* and *G″* increased further (Figure S8, Supporting Information). The gelation was complete after 16 h at pH 3.3. **3** had more unusual gelation kinetics; this could be due to the molecule having two apparent pK_as (Figure S9b, Supporting Information), unlike the other two gelators which only have one. The sample started to assemble at pH 7.4 after 1 min, where the pH was around the first pK_a of the gelator. *G′* and *G″* then plateau at around 100 min and pH 5.6, the second pK_a of the gelator. After this point, the pH continues to decrease. *G′* and *G″* also decrease before increasing again at pH 5 at around 300 min (Figure 2b; Figure S9, Supporting Information). *G′* and *G″* finish increasing after 33 h where the gel has a final pH of 4.2. These different stages in the gelation can be linked to fiber entanglement, associations or even rearrangement, but are still not fully understood.[2b,18] pK_a and gelation kinetics are important when designing coassembled or self-sorted systems.[9] Changes in structure of the gel during gelation could be monitored and explored further with the use of kinetic SAXS experiments, NMR and kinetic UV–vis absorption experiments. As we are interested in the end properties of our gels we have not investigated this further.

We again characterized the gels using SAXS and SEM. The fits to the SAXS data imply that the gels are formed by the entanglement of long anisotropic structures in each case. The scattering data from a gel of **1** can be fitted to a cylinder model (Figure S2a, Supporting Information), although polydispersity has to be incorporated for a satisfactory fit. The fit implies that the radius is 3.41 ± 0.24 nm, with a polydispersity of 0.61, with a length of 387.5 ± 23.7 nm. The scattering data for the gel of **2** (Figure S2b, Supporting Information) is best fitted to an elliptical cylinder with a radius of 3.24 ± 0.03 nm, a radius ratio of 4.07 ± 0.01, and a length of 418.4 ± 30.2 nm. The data for the gel of **2** fits best to a model that combines a power law and a cylinder. Alternatives such as the flexible cylinder model, elliptical cylinder, or hollow cylinder (in all cases with or without a power law component) do not adequately capture the data. The fit suggests that the cylinders have a radius of 3.42 ± 0.05 nm, with a length of 136.2 ± 7.8 nm. The gel of **3** scatters much more strongly than the solution (Figure S2c, Supporting Information). The data can be fitted to a flexible cylinder model, although again polydispersity needs to be included in the radius to capture the data effectively. The fit implies that the radius is 3.06 ± 0.11 nm, with a polydispersity of 0.31. The Kuhn length is 5.58 ± 0.63 nm, with the length being 303.6 ± 4.3 nm. Again, the quality of the fit is relatively insensitive to the length.

SEM images show that all the gels consist of a fibrous network. The SEM images for gel **1** shows an entangled network with fibre diameters of 24 ± 5 nm, which are more than double the diameters expected from the fits to the SAXS data (Figure S10a–c Supporting Information). This could be due to

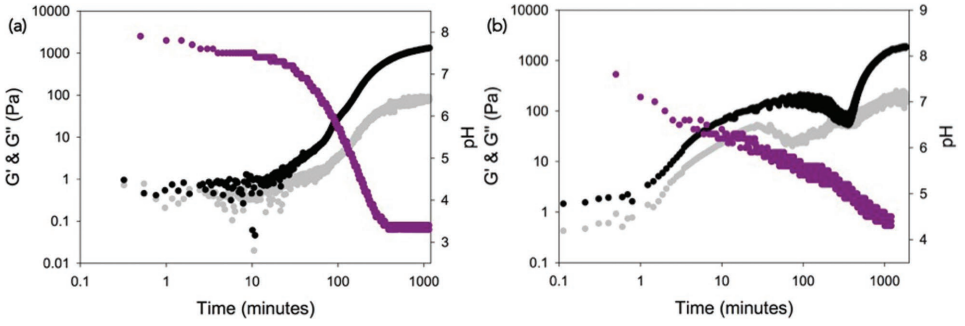

Figure 2. The development of rheological measurements and change in pH during gelation of a) 1 and b) 3. The black data represent *G′* and gray data represent *G″*. Purple data represent pH data. Rheology was recorded at 25 °C at a strain of 0.5% and a frequency of 10 rad s^{-1}.

aggregation upon drying,[16] or because the SAXS is not sensitive to the larger structures, but rather the primary fibers. Gel **2** however showed bundles of fibers, which again could be a result of drying (Figure S10b, Supporting Information).[16]

UV–vis absorption spectra were collected for the solutions, dried solutions, gels, and xerogels. In solution, **1** has a peak at 410 nm with a shoulder at 440 nm (Figure S11a, Supporting Information). When gelled, these peaks broaden due to increased aggregation; again, this is typical for many such gelators.[19] Interestingly, new peaks are formed at 650 and 1000 nm. This results in a visual change from a yellow/brown solution to a dark green gel. The literature suggests this could be from the production of the radical cation.[20] To investigate this further, the gel was irradiated with a 410 nm LED for 10 min. These peaks increased in intensity, suggesting they were from the radical cation formation and daylight was enough to form the radical cation to some degree (**Figure 3**a). Electron paramagnetic resonance (EPR) spectroscopy was performed on the gels to further support the presence of the radical cation (Figure 3b). EPR showed the presence of radical anion with no defined splitting meaning it was delocalized over the molecule. When the solution of **1** was irradiated for 10 min, no extra peaks were seen in the UV–vis absorption spectrum, but the EPR showed a very small amount of radical present in solution. The amount of radical present in solution compared to that of the gel was 3%. (Figure S12, Supporting Information). The viscosity and SAXS data show there is little structure at high pH, but when the pH is lowered to form the gel persistent structures are formed. It therefore appears that the ability to form the radical cation photochemically depends on the aggregation state of the molecules, linking with previous observations.[21] This is further demonstrated by drying; when the solution of **1** is dried to form a thin film, the peaks again broaden, red shift and a shoulder peak at 390 nm is now visible (Figure S11b, Supporting Information). Like the wet gel, a peak at 650 nm appears on drying, suggesting that the radical cation in stable in the wet gel and dried film, but not the solution.

In the solution of **2**, there are three peaks at 470, 390, and 300 nm (Figure S13a, Supporting Information). Upon gelation, these peaks red shift slightly, again suggesting H-type aggregation. When dried to a thin film or a xerogel, the peaks are in the same position but the peaks are broader due to drying effects (Figure S13b, Supporting Information). The small change in the spectra agrees with the viscosity and SAXS data, which showed similar structures at both high and low pH. The solution of **3** has a peak 380 nm as does the dried solution of **3** (Figure S14, Supporting Information). On gelation, there is an additional shoulder peak at 420 nm for both the wet gel and xerogel. This suggests there is a change in aggregation from the solution to gel, which agrees with the viscosity and SAXS data, which also show there is little structure at high pH and then fibers at low pH.

The conductivity of each xerogel and dried solution was measured using a 2 electrode IV experiment, where the voltage is changed and the current across the sample measured.[22] 10 μL of either the solution or gel was dried in a 3 mm × 3 mm mask to form a thin film of material. Silver electrodes were placed either side of the sample and attached to copper wire, which were connected to a potentiostat. The current was then measured between −4 and 4 V. Prior to the measurements, the quality of all of the films was determined by imaging the samples using cross-polarized optical microscopy to ensure a contiguous pathway. All of the samples showed Ohmic contact and were highly resistive as expected. To test their suitability as p-type materials, the current was measured again after the samples had been doped by exposure to an atmosphere of iodine (Figures S15–S17, Supporting Information).[14j,15b] All of the samples showed a similar decrease in resistivity upon exposure to iodine vapor. The dried solutions showed a greater response to the iodine in all of the samples (**Figure 4**a,b). We have seen similar behavior with n-type materials such as perylene diimides where the dried solutions showed higher conductivity than the dried gels, which we have attributed to the solutions containing more aligned structures than the gels. However, the differences could also be due to the more entangled, dense nature of the fibers in the gels meaning that the iodine cannot fully penetrate the dried network.[22] The dried solution of **2** showed the greatest response to iodine by two orders of magnitude, suggesting this sample could act as an effective p-type material (Figure 4a). The solution of **2** may have shown the greatest response as it had worm-like micelles present in solution, unlike **1** and **3**. The worm-like micelles would provide a continuous path for the electrons to travel, whereas the samples with no structures present it would be more

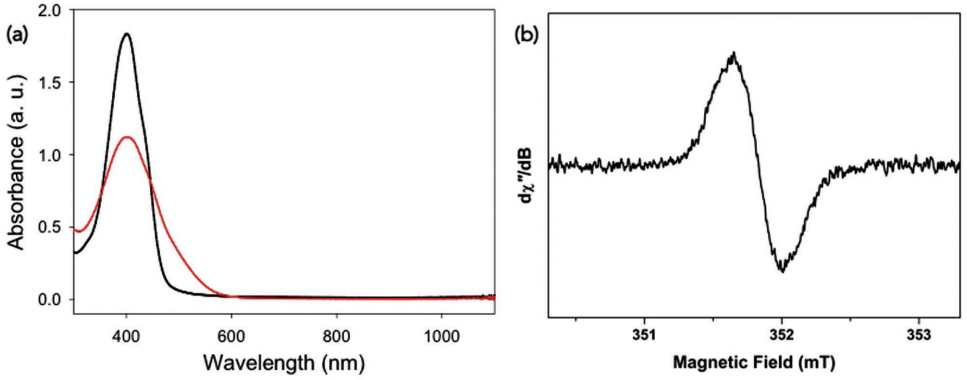

Figure 3. a) UV–vis absorption spectra of xerogel 1 before irradiation (black data) and after irradiation for 10 min with 410 nm LED (red data). b) X-band EPR spectrum of gel 1 in aqueous solution at 293 K (experimental conditions: 9.8641 GHz; power, 2.0 mW; modulation, 0.2 mT).

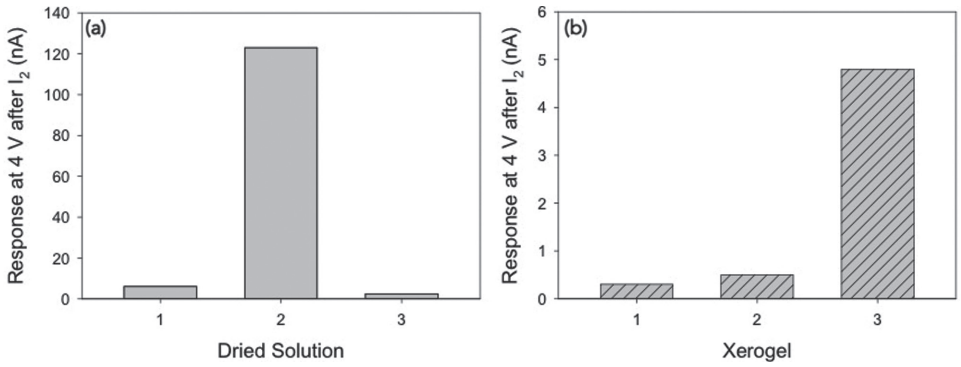

Figure 4. Response at 4 V from a) dried solutions and b) xerogels of 1, 2, and 3 after being exposed to iodine vapor.

difficult for the electrons to travel through the sample. This would lead to a recombination of the charges rather than conductivity. Xerogel **3** showed the greatest response for the gel samples. This may be due to the morphology of the fibers. Xerogels **1** and **2** fit to cylinder models from the SAXS, whereas xerogel **3** fits to a flexible cylinder model. However, we again highlight that the conductivity for the xerogels is significantly lower than for the dried solutions. Comparing to similar systems is however difficult, as the experiment set up can alter the results dramatically. The Ulijn group have prepared a TTF-based organogel, which was found to have a conductivity of 4 nA at 4 V upon exposure to iodine.[14j] Our TTF-based gel (gel **2**) shows a value less than this, as does gel **1**, but gel **3** shows similar values. The solutions however all show similar or greater conductivities than the TTF organogel, and in the case of the solution of **2**, significantly greater conductivities. Again, directly comparing with other values in the literature if difficult, but we can clearly see from our data that the solutions are more conductive than our xerogels.

4. Conclusions

We have prepared new amino acid functionalized p-type gelators based on oligo(phenylenevinylene), tetrathiafulvalenes, and terthiophene cores. Gelation was achieved using a slow pH drop with the hydrolysis of GdL, resulting in highly reproducible gels as shown in the rheological data. When dried into films, all of the samples showed improved conductivity upon exposure to iodine as either dried solutions or xerogels, showing they have some p-type behavior. The solutions in general had a better response than the corresponding xerogels, with **2** being the most responsive solution. This could be due to **2** having worm-like micelles present in solution, as seen by scattering, optical microscopy, and SEM and so having a more continuous path for charges to travel along with less chance of recombination. The xerogels do have these fibers as seen in the scattering data, but from the SEM it can be seen these are not ordered and are randomly orientated and so there is not a direct path for charges, and so increasing the chance of recombination. With the fibrous network being entangled, it could also be that the iodine could not diffuse effectively into the film. Overall, these three new hydrogelators show potential to be used in p-type systems, and could further be potentially used in p–n systems tuned by using an appropriate n-type hydrogelator and designing and controlling the gelation carefully. The terthiophene based gelator was able to form a highly stable radical cation in both the wet gel and the xerogel. This stable radical cation is stabilized by the aggregation of the molecules and is not formed in the solution, showing how important the local molecular packing is for tuning the properties of the self-assembled aggregates. This easily formed stable radical cation could be further used in reactions as well as in electronic materials.

Supporting Information

Supporting Information is available from the Wiley Online Library or from the author.

Acknowledgements

E.R.D. thanks the Leverhulme Trust for an Early Career fellowship (ECR-2017-223) and the University of Glasgow for a LKAS Leadership Award. D.J.A. thanks the EPSRC for a fellowship, (EP/L021978/1). The Ganesha X-ray scattering apparatus used for this research was purchased under EPSRC Grant "Atoms to Applications" (Grant ref. EP/K035746/1).

Conflict of Interest

The authors declare no conflict of interest.

Keywords

hydrogels, oligo phenylene vinylenes, self-assembly, terthiophenes, tetrathiafulvalenes

Received: November 2, 2017
Revised: December 5, 2017
Published online:

[1] Z. Wang, P. K. Nayak, J. A. Caraveo-Frescas, H. N. Alshareef, *Adv. Mater.* **2016**, *28*, 3831.

[2] a) P. Terech, R. G. Weiss, *Chem. Rev.* **1997**, *97*, 3133; b) E. R. Draper, D. J. Adams, *Chem* **2017**, *3*, 390; c) M. de Loos, B. L. Feringa, J. H. van Esch, *Eur. J. Org. Chem.* **2005**, *2005*, 3615; d) S. S. Babu, S. Prasanthkumar, A. Ajayaghosh, *Angew. Chem., Int. Ed.* **2012**, *51*, 1766; e) S. S. Babu, K. K. Kartha, A. Ajayaghosh, *J. Phys. Chem. Lett.* **2010**, *1*, 3413; f) F. J. M. Hoeben, P. Jonkheijm, E. W. Meijer, A. P. H. J. Schenning, *Chem. Rev.* **2005**, *105*, 1491; g) F. Würthner, Z. Chen, F. J. M. Hoeben, P. Osswald, C.-C. You, P. Jonkheijm, J. v. Herrikhuyzen, A. P. H. J. Schenning, P. P. A. M. van der Schoot, E. W. Meijer, E. H. A. Beckers, S. C. J. Meskers, R. A. J. Janssen, *J. Am. Chem. Soc.* **2004**, *126*, 10611; h) S. Ghosh, V. K. Praveen, A. Ajayaghosh, *Annu. Rev. Mater. Res.* **2016**, *46*, 235; i) S. Ghosh, S. Cherumukkil, C. H. Suresh, A. Ajayaghosh, *Adv. Mater.* **2017**, *29*, 1703783.

[3] a) H. A. M. Ardoña, J. D. Tovar, *Bioconjugate Chem.* **2015**, *26*, 2290; b) T. Kitahara, M. Shirakawa, S.-i. Kawano, U. Beginn, N. Fujita, S. Shinkai, *J. Am. Chem. Soc.* **2005**, *127*, 14980; c) H. Su, Y. Wang, C. F. Anderson, J. M. Koo, H. Wang, H. Cui, *Chin. J. Polym. Sci.* **2017**, *35*, 1194; d) D. B. Amabilino, J. Puigmarti-Luis, *Soft Matter* **2010**, *6*, 1605; e) H. Xu, A. K. Das, M. Horie, M. S. Shaik, A. M. Smith, Y. Luo, X. Lu, R. Collins, S. Y. Liem, A. Song, P. L. A. Popelier, M. L. Turner, P. Xiao, I. A. Kinloch, R. V. Ulijn, *Nanoscale* **2010**, *2*, 960.

[4] E. R. Draper, O. O. Mykhaylyk, D. J. Adams, *Chem. Commun.* **2016**, *52*, 6934.

[5] a) E. R. Draper, E. G. B. Eden, T. O. McDonald, D. J. Adams, *Nat. Chem.* **2015**, *7*, 848; b) D. J. Cornwell, B. O. Okesola, D. K. Smith, *Angew. Chem., Int. Ed.* **2014**, *53*, 12461; c) S. Strandman, X. X. Zhu, *Gels* **2016**, *2*, 16.

[6] a) J. Raeburn, C. Mendoza-Cuenca, B. N. Cattoz, M. A. Little, A. E. Terry, A. Zamith Cardoso, P. C. Griffiths, D. J. Adams, *Soft Matter* **2015**, *11*, 927; b) E. R. Draper, L. L. E. Mears, A. M. Castilla, S. M. King, T. O. McDonald, R. Akhtar, D. J. Adams, *RSC Adv.* **2015**, *5*, 95369.

[7] J. Raeburn, A. Zamith Cardoso, D. J. Adams, *Chem. Soc. Rev.* **2013**, *42*, 5143.

[8] a) D. J. Adams, M. F. Butler, W. J. Frith, M. Kirkland, L. Mullen, P. Sanderson, *Soft Matter* **2009**, *5*, 1856; b) Y. Pocker, E. Green, *J. Am. Chem. Soc.* **1973**, *95*, 113.

[9] J. Raeburn, D. J. Adams, *Chem. Commun.* **2015**, *51*, 5170.

[10] a) C. Colquhoun, E. R. Draper, E. G. B. Eden, B. N. Cattoz, K. L. Morris, L. Chen, T. O. McDonald, A. E. Terry, P. C. Griffiths, L. C. Serpell, D. J. Adams, *Nanoscale* **2014**, *6*, 13719; b) K. L. Morris, L. Chen, J. Raeburn, O. R. Sellick, P. Cotanda, A. Paul, P. C. Griffiths, S. M. King, R. K. O'Reilly, L. C. Serpell, D. J. Adams, *Nat. Commun.* **2013**, *4*, 1480.

[11] E. R. Draper, J. R. Lee, M. Wallace, F. Jackel, A. J. Cowan, D. J. Adams, *Chem. Sci.* **2016**, *7*, 6499.

[12] E. R. Draper, M. Wallace, R. Schweins, R. J. Poole, D. J. Adams, *Langmuir* **2017**, *33*, 2387.

[13] K. Sugiyasu, S.-i. Kawano, N. Fujita, S. Shinkai, *Chem. Mater.* **2008**, *20*, 2863.

[14] a) A. Ajayaghosh, S. J. George, *J. Am. Chem. Soc.* **2001**, *123*, 5148; b) S. J. George, A. Ajayaghosh, *Chem. - Eur. J.* **2005**, *11*, 3217; c) S. J. George, A. Ajayaghosh, P. Jonkheijm, A. P. H. J. Schenning, E. W. Meijer, *Angew. Chem., Int. Ed.* **2004**, *43*, 3422; d) X. Yang, D. Zhang, G. Zhang, D. Zhu, *Sci. China Chem.* **2011**, *54*, 596; e) X. Yang, G. Zhang, L. Li, D. Zhang, L. Chi, D. Zhu, *Small* **2012**, *8*, 578; f) C. Yu, M. Xue, K. Liu, G. Wang, Y. Fang, *Langmuir* **2014**, *30*, 1257; g) S. Prasanthkumar, A. Gopal, A. Ajayaghosh, *J. Am. Chem. Soc.* **2010**, *132*, 13206; h) S. Prasanthkumar, S. Ghosh, V. C. Nair, A. Saeki, S. Seki, A. Ajayaghosh, *Angew. Chem., Int. Ed.* **2015**, *54*, 946; i) D. A. Stone, A. S. Tayi, J. E. Goldberger, L. C. Palmer, S. I. Stupp, *Chem. Commun.* **2011**, *47*, 5702; j) S. K. M. Nalluri, N. Shivarova, A. L. Kanibolotsky, M. Zelzer, S. Gupta, P. W. J. M. Frederix, P. J. Skabara, H. Gleskova, R. V. Ulijn, *Langmuir* **2014**, *30*, 12429.

[15] a) J. López-Andarias, M. J. Rodriguez, C. Atienza, J. L. López, T. Mikie, S. Casado, S. Seki, J. L. Carrascosa, N. Martín, *J. Am. Chem. Soc.* **2015**, *137*, 893; b) E. R. Draper, B. Dietrich, D. J. Adams, *Chem. Commun.* **2017**, *53*, 1864; c) H. A. M. Ardona, K. Besar, M. Togninalli, H. E. Katz, J. D. Tovar, *J. Mater. Chem. C* **2015**, *3*, 6505; d) A. M. Castilla, E. R. Draper, M. C. Nolan, C. Brasnett, A. Seddon, L. L. E. Mears, N. Cowieson, D. J. Adams, *Sci. Rep.* **2017**, *7*, 8380.

[16] L. L. E. Mears, E. R. Draper, A. M. Castilla, H. Su, Zhuola, B. Dietrich, M. C. Nolan, G. N. Smith, J. Doutch, S. Rogers, R. Akhtar, H. Cui, D. J. Adams, *Biomacromolecules* **2017**, *18*, 3531.

[17] a) L. Chen, K. Morris, A. Laybourn, D. Elias, M. R. Hicks, A. Rodger, L. Serpell, D. J. Adams, *Langmuir* **2010**, *26*, 5232; b) P. R. A. Chivers, D. K. Smith, *Chem. Sci.* **2017**, *8*, 7218.

[18] R. G. Weiss, *J. Am. Chem. Soc.* **2014**, *136*, 7519.

[19] T. H. Kim, M. S. Choi, B.-H. Sohn, S.-Y. Park, W. S. Lyoo, T. S. Lee, *Chem. Commun.* **2008**, 2364.

[20] a) D. Yamazaki, T. Nishinaga, N. Tanino, K. Komatsu, *J. Am. Chem. Soc.* **2006**, *128*, 14470; b) V. Wintgens, P. Valat, F. Garnier, *J. Phys. Chem.* **1994**, *98*, 228.

[21] L. L. Miller, K. R. Mann, *Acc. Chem. Res.* **1996**, *29*, 417.

[22] E. R. Draper, J. J. Walsh, T. O. McDonald, M. A. Zwijnenburg, P. J. Cameron, A. J. Cowan, D. J. Adams, *J. Mater. Chem. C* **2014**, *2*, 5570.

